

Hydrogeochemistry and rare earth element behavior in a volcanically acidified watershed in Patagonia, Argentina

Christopher H. Gammons^{a,*}, Scott A. Wood^b, Fernando Pedrozo^c,
Johan C. Varekamp^d, Bethany J. Nelson^b, Christopher L. Shope^a, Gustavo Baffico^e

^a*Department of Geological Engineering, Montana Tech of The University of Montana, Butte, MT 59701, United States*

^b*University of Idaho, Moscow, ID, United States*

^c*Universidad del Comahue, Bariloche, Argentina*

^d*Wesleyan University, Middletown, CT, United States*

^e*CONICET, Argentina*

Received 10 January 2005; received in revised form 9 May 2005; accepted 8 June 2005

Abstract

The Rio Agrio watershed in northern Patagonia, Argentina is naturally acidic due to discharges of volcanic H₂SO₄, HCl, and HF at its headwaters near the summit of Copahue Volcano. A suite of water samples was collected from the summit of the volcano to a point roughly 40 km downstream where the pH of the Rio Agrio rose above 6.0. This suite included a sample of the hyperacidic (pH<1) crater lake at the summit of Copahue, the hot-spring source of the Upper Rio Agrio (pH<2), two depth profiles through Lake Caviahue (a large glacially-carved lake with pH~2.6, located 10 km east of the volcano summit), and several samples of the Lower Rio Agrio downstream of Lake Caviahue where pH increased due to the influx of tributary streams. Both filtered and non-filtered samples were collected and analyzed for major ions, trace metals, and rare earth elements (REE).

The concentrations of REE in the Rio Agrio decreased by several orders of magnitude through the study area, as a result of dilution and chemical attenuation. A subtle shift in the slope of shale-normalized profiles of dissolved REE concentration was observed, from being weakly positive near the source of the Rio Agrio, to showing a weak middle REE enrichment trend in Lake Caviahue, to being weakly negative in the lower reaches of the river. The trend to a negative slope across the lanthanide series in the lower river is explained by selective partitioning of the heavier REE to hydrous oxides of Fe and Al suspended in the water column, and accumulating on the riverbed. Most of the decrease in REE load occurred immediately downstream of the confluence with a tributary that increased the pH of the Rio Agrio from 4.3 to 6.1. Although the mixed water was supersaturated with REE phosphate compounds, precipitation of LnPO₄ is not believed to have been a dominant process because the predicted pattern of inter-element fractionation from phosphate deposition is inconsistent with the observed trends. Instead, REE attenuation most

* Corresponding author.

E-mail address: cgammons@mttech.edu (C.H. Gammons).

likely occurred from adsorption onto freshly precipitated hydrous aluminum oxide. The behavior of REE in the Rio Agrio watershed is broadly similar to what has been observed in watersheds that owe their acidity to oxidation of sulfide minerals. © 2005 Elsevier B.V. All rights reserved.

Keywords: Rare earth elements; Geochemistry; Limnology; Crater lake; Adsorption; Acid rock drainage; Argentina

1. Introduction

The geochemistry of rare earth elements (REE) in acidic surface waters has been the focus of many recent investigations (Johannesson and Lyons, 1995; Johannesson et al., 1996; Lewis et al., 1997; Elbaz-Poulichet and Dupuy, 1999; Johannesson and Zhou, 1999; Gimeno et al., 2000; Leybourne et al., 2000; Åström, 2001; Worrall and Pearson, 2001a,b; Gammons et al., 2003, 2005; Verplanck et al., 2004; Bozau et al., 2004; Wood et al., 2005). Because different rock types typically have distinctive REE profiles, the REE are often used by geochemists as fingerprints of source regions. However, in low temperature aqueous environments, subtle differences in electronic configuration across the lanthanide series lead to differences in the behavior of REE with respect to aqueous complexation, ion adsorption, and mineral precipitation. Because of these differences, the REE may be fractionated during weathering and solute transport, leading to changes in the REE profiles in both solid and aqueous media. Although these fractionation processes are more pronounced in near-neutral or alkaline waters where the REE solubilities are low, REE fractionation has also been reported in acidic waters. For example, a number of studies have reported enrichments of the middle REE (relative to North American Shale Composite, or NASC) in lakes, rivers, and groundwaters with low pH (Johannesson et al., 1996; Elbaz-Poulichet and Dupuy, 1999; Johannesson and Zhou, 1999; Gimeno et al., 2000; Leybourne et al., 2000; Worrall and Pearson, 2001a,b). However, recent investigations have shown that contrary trends exist in acidic waters, including light REE enrichment (Bozau et al., 2004; Gammons et al., *in press*), heavy REE enrichment (Gammons et al., 2003), and middle REE depletion (Verplanck et al., 2004). Thus, it cannot be said that there is a general REE pattern that is universally characteristic of low pH waters.

Most previous studies of REE in acidic waters have focused on mining-impacted streams and lakes (e.g., Elbaz-Poulichet and Dupuy, 1999; Gimeno et al., 2000;

Leybourne et al., 2000; Åström, 2001; Worrall and Pearson, 2001a,b; Gammons et al., 2003, 2005; Verplanck et al., 2004; Bozau et al., 2004; Wood et al., 2005), or acid hot springs (Kikawada et al., 1993; Lewis et al., 1997; Wood, 2003). In contrast, there have been relatively few studies of REE in naturally-acidic lakes (Johannesson and Lyons, 1995; Johannesson and Zhou, 1999; Takano et al., 2004), and we are not aware of a previous investigation of REE in a naturally-acidic river. The focus of the present study is the Rio Agrio watershed, a drainage basin in northwest Patagonia, Argentina. This watershed owes its acidity to volcanic inputs of HCl, HF, and H₂SO₄ at the headwaters of the river, which occur as a series of hot springs on the east flank of Copahue Volcano (Goss, 2001; Varekamp et al., 2001, 2004, *in press*; Wendt-Potthoff and Koschorreck, 2002). Copahue is an active stratovolcano (el. 2965 m) of predominantly andesitic composition, whose most recent eruption was during July–August of 2000 (Varekamp et al., 2001). Although the Rio Agrio is diluted by several tributary streams, it remains acidic for more than 40 km downgradient from its hot-spring source (Fig. 1). Besides the Rio Agrio itself, the watershed includes a hyperacidic (pH < 1) volcanic crater lake, and a much larger glacially-carved lake occupying a portion of the floor of an old caldera (Pedrozo et al., 2001). Because of these unique features, the Copahue/Rio Agrio system affords an opportunity to examine the behavior of rare earth elements in a variety of lotic and limnic settings, all within a watershed that is naturally acidic. The results of this study provide an interesting contrast to investigations of REE in mining-impacted watersheds, and should be of interest to anyone dealing with the geochemistry of REE in acidic waters.

2. Methods

2.1. Field methods

Most of the water samples reported in this study were collected during March 20 to 24, 2003. Addi-

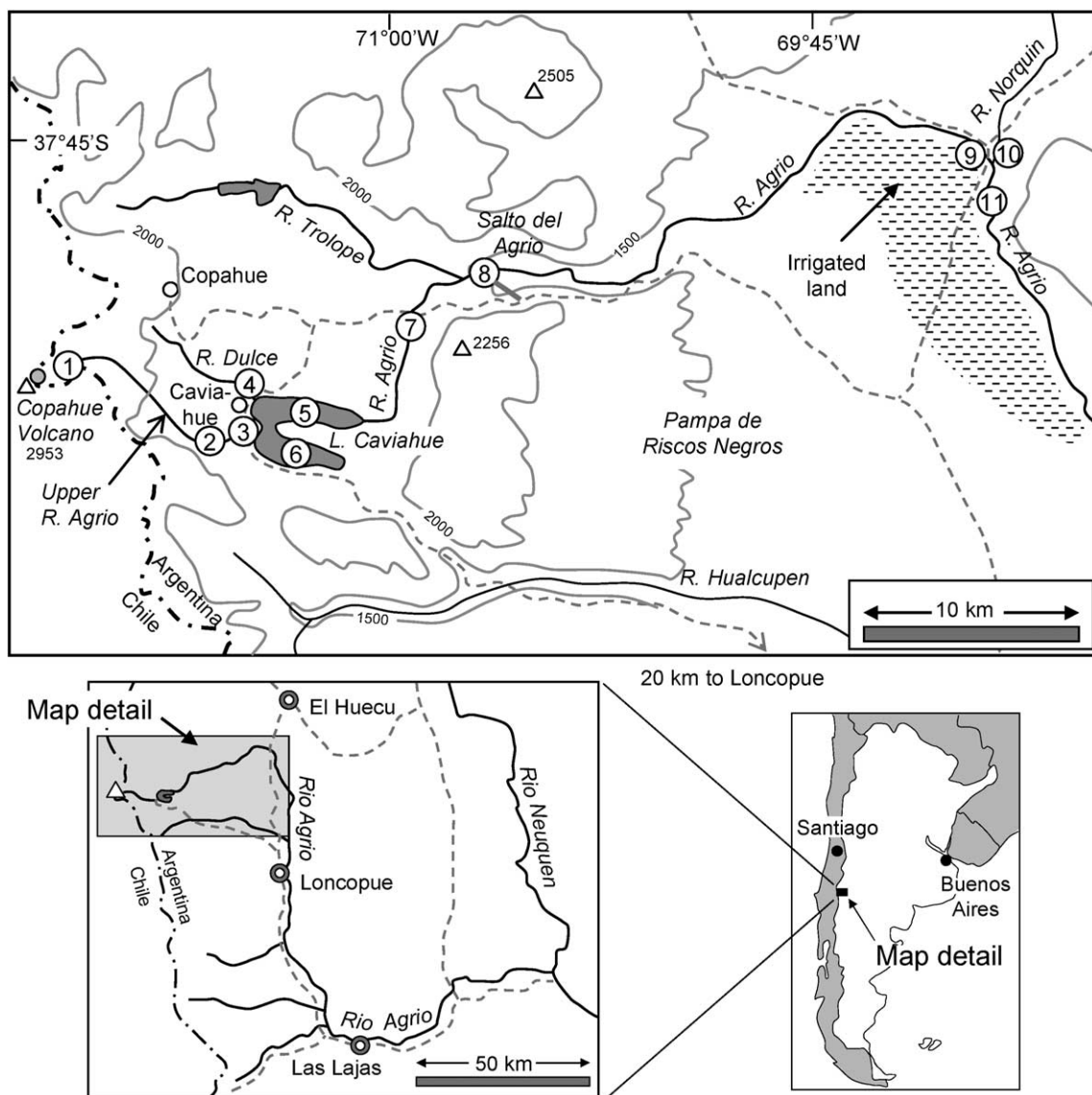


Fig. 1. Location map of the Rio Agrio watershed, showing the major topographical features and sampling sites. Roads are dashed gray lines, rivers are black lines, and elevation contours (in meters) are thin gray lines. The dot-dashed line is the Chile–Argentina border, and corresponds to the Continental Divide of this portion of the Andes Mountains. Insets show the entire Rio Agrio watershed in Neuquen Province and the location within Argentina.

tional samples from the Copahue crater lake and the hot-spring source of the Rio Agrio were collected on March 15, 1997. During this time of year (late summer), rivers in Patagonia are typically near their lowest annual discharge, and weather is optimal for fieldwork. At each sampling location, pH, water temperature (T), specific conductance (SC), dissolved

oxygen (DO), and electrical potential (Eh) were measured using WTW 304i and Orion 1230 portable multimeters. All electrodes were calibrated at least once daily: the DO electrode was calibrated immediately before each measurement. Calibration of pH was performed with pH 2, 4 and 7 standards, whereas Eh was calibrated with pH 4 and pH 7 quinhydrone

standards. All Eh measurements reported in this paper have been corrected to the standard hydrogen electrode. All SC measurements are referenced to 25 °C. Acidity and alkalinity titrations were performed on pre-filtered samples within 12 h of sample collection. Acidity titrations were performed to a pH endpoint of 8.4, whereas alkalinity was titrated to an endpoint of 4.5.

Paired filtered and non-filtered water samples were collected at each station. Filtration was accomplished using a hand-operated peristaltic pump and 47-mm diameter Metricel® membrane filters (pore size 0.45- μ m). At least 30 mL of water were passed through a new filter before a sample was collected, and at least 30 mL of distilled water were passed through the unit between samples. Two non-filtered blanks were transported with the field samples to Argentina and were opened to the atmosphere for ~1 min at the time that samples were collected. All samples were stored in 250 mL polypropylene bottles that were washed by soaking overnight in a mixture of reagent-grade 5% HNO₃–5% HCl, followed by soaking overnight in a mixture of high-purity (Fisher Optima) 5% HNO₃–5% HCl, and finally rinsed at least five times with 18-M Ω -cm deionized water. The washed bottles were placed into clean Ziplock® bags for transport to and from the field. All samples collected in 2003 were acidified in the field laboratory to 5% with Fisher Optima grade nitric acid. The field blanks were acidified in the same manner as the river samples. Samples of water from Lake Caviahue (Fig. 1) were collected from a rubber Zodiac boat using a Van Dorn sampler and an electric winch. Field parameters (*T*, SC, pH, Eh, DO) were obtained immediately upon bringing each water sample to the surface. Water samples collected in 1997 were filtered to 0.45 μ m but were not acidified, as the samples had a pH < 0.5 with no acidification.

2.2. Analytical methods

Unacidified samples were analyzed using a Dionex AI-450 ion chromatography (IC) workstation to determine the concentrations of the anions fluoride, chloride, bromide, nitrate, sulfate, and phosphate. An isocratic elution with a sodium bicarbonate–sodium carbonate eluent was employed together with a Dionex AS4-SC column. Although standards were

prepared containing only the above anions, other anions would have been detected if present at levels greater than approximately 0.1 mg/L. For the more concentrated samples, dilution was required for reliable anion analysis.

Concentrations of As, Al, Ba, Ca, Fe, K, Mg, Mn, Na, P, Rb, Si, Sr, and Zn in acidified samples (filtered and unfiltered) and field blanks were determined using a Perkin-Elmer Optima 3000-XL inductively coupled plasma-atomic emission spectrometer (ICP-AES) equipped with an axial torch. A conservative limit of detection for these metals is about 5–10 μ g/L. All calibration standards, blanks, and quality control standards were matrix-matched to the samples with respect to acid concentration. The elements B, Co, Cu, Li, Mo, Ni, Pb, Ti, V, and W were also determined by ICP-AES, but are not reported here. Some of these elements (e.g., Mo, Pb, W) were below the detection limit in almost all samples, and the remainder were below or only slightly above the detection limits in most samples.

For the 2003 sample set, the concentrations of all REE except Pm were determined at Washington State University using a *ThermoFinnigan Element 2* inductively coupled plasma-mass spectrometer (ICP-MS). Pre-concentration was not required for analysis of any samples, but samples with lower pH and higher total dissolved solids required dilution. Indium and rhenium were used as internal standards. The following masses were monitored: ¹³⁹La, ¹⁴⁰Ce, ¹⁴¹Pr, ¹⁴⁶Nd, ¹⁴⁷Sm, ¹⁵¹Eu, ¹⁶⁰Gd, ¹⁵⁹Tb, ¹⁶³Dy, ¹⁶⁵Ho, ¹⁶⁶Er, ¹⁶⁹Tm, ¹⁷⁴Yb, and ¹⁷⁵Lu. The masses were selected and the forward power and argon flow rates for the plasma were adjusted to minimize isobaric oxide interferences. However, corrections were made for ¹⁵¹Eu due to ¹³⁵Ba¹⁶O interference in all samples, and for ¹⁵⁹Tb due to interference from ¹⁴¹Pr¹⁸O in most of the samples. The ICP-MS was calibrated using standards containing 0.08, 0.4, 2, and 8 μ g/L of each REE. Quality control was maintained by analyzing two mid-level standards and a blank every 10 samples in the analysis. Data were reprocessed offline using a standardized spreadsheet. Instrument detection limits (IDL) were determined by analyzing 10 instrument blanks (acidified 18-M Ω -cm deionized water). The standard deviation of instrument-blank concentrations for each analyte was multiplied by the Student's *t* (2.821) at the 99% confidence level to calculate the

IDL, which ranged from approximately 0.2 to 1.9 ng/L depending on the REE.

Rock samples from Copahue Volcano were crushed to a powder with an Al-ceramic mini-jaw crusher followed by a shatterbox with Al-ceramic disc and liner. The powdered rock samples, as well as water samples collected in 1997, were submitted to XRAL Laboratories (Toronto, Canada) for REE analysis by ICP-MS. The rocks were prepared by fusion with Na₂O₂, followed by dissolution in a mix of strong acids.

2.3. Modeling

The geochemical modeling program Visual MINTEQ (Version 2.2, a recent adaptation of the original code written by Allison et al., 1991) was used to calculate the equilibrium aqueous speciation of REE and other solutes, as well as saturation indices for relevant solids, in the Upper and Lower Rio Agrio. The Visual MINTEQ database contains thermodynamic data for most of the common REE solids (oxides, hydroxides, carbonates, phosphates, and fluorides), as well as the principal aqueous species (complexes with carbonate, sulfate, fluoride, and hydroxide ligands). The database was amended to include recent thermodynamic data on the 1:1 REE-carbonate (Liu and Byrne, 1998), REE-sulfate (Schijf and Byrne, 2004), and REE-hydroxide (Klungness and Byrne, 2000) complexes.

3. Results

Table 1 provides a list of the sampling sites, along with field parameters and anion concentrations measured in March 2003. Analytical data for major and trace metals are given in Appendix A, and all REE data are tabulated in Appendices B, C, and D.

3.1. General hydrogeochemical trends

3.1.1. Copahue crater lake

During our March 2003 visit, dangerous ground and intense acid vapors made it impossible to collect a water sample from the crater lake at the summit of Copahue Volcano. Previous chemical analyses (Varekamp et al., 2001, 2004) indicate that the lake is hyperacidic (pH 0.18 to 0.30) and warm (21 to 54 °C at surface), with extremely high concentrations of Cl, SO₄, and rock-forming elements. An early sample collected by the Wesleyan group in March 1997 was used for the REE analyses reported below. Although the crater lake sits directly on top of a shallow, actively degassing magma chamber, the chemistry of the lake is also influenced by direct precipitation and melting of summit glaciers and snowpack. In addition, the water level and chemistry of the crater lake fluctuate drastically from season to season and year to year, depending on climate and the current state of volcanic activity. For these reasons, the hot-spring source of the Upper Rio Agrio (see below) is believed

Table 1
Field parameters and anion analyses for water samples from the Rio Agrio watershed

Site	Date	Description	T (°C)	pH	SC (μS/cm)	Eh (mV)	Cl (mg/L)	F (mg/L)	SO ₄ (mg/L)	Acid/alk (meq/L)
1	3/20/03	U. Agrio source	67.5	1.55 ^a	32300 ^a	616	9850	737	14700	27.5 (acid)
2	3/20/03	U. Agrio above tributary	14.9	2.28	5710	672	821	68	1470	2.52 (acid)
3	3/20/03	U. Agrio at mouth	15.3	2.43	5260	673	760	63	1420	0.41 (acid)
4	3/22/03	R. Dulce	16.5	6.69	307	n.a.	19	0.68	90	0.16 (alk)
5 ^b	3/22/03	N. Arm, Caviahue Lake	15.8	2.65	1640	n.a.	76	6.6	408	n.a.
6 ^b	3/22/03	S. Arm, Caviahue Lake	15.2	2.68	1650	793	73	6.7	391	n.a.
7	3/20/03	L. Agrio below lake	12.0	2.76	1220	743	54	3.7	286	n.a.
8	3/23/03	L. Agrio above Salto	12.9	3.19	562	737	24	1.9	135	n.a.
9	3/23/03	L. Agrio above Norquin	14.7	4.67	317	592	19	0.94	104	n.a.
10	3/23/03	R. Norquin	18.1	8.41	300	434	5.5	0.26	25	2.30 (alk)
11	3/23/03	L. Agrio below Norquin	15.4	6.09	300	473	17.6	0.75	85	0.26 (alk)
12	3/24/03	L. Agrio at Loncapue	12.2	8.30	201	484	6.96	0.32	39	0.88 (alk)

T=temperature, SC=specific conductance, Eh=electrical potential, acid=acidity, alk=alkalinity, n.a.=not analyzed.

^a After cooled to room temperature, pH=1.43, SC=41,300.

^b Collected at a depth of 5 m below surface.

to be more representative of the deep volcanic hydrothermal system (Varekamp et al., 2001, 2004).

3.1.2. Upper Rio Agrio

The Upper Rio Agrio begins as a hot spring (Site 1) high on Copahue Volcano (el. 2740 m). Prior to the July 2000 eruption, this hot spring was hyperacidic, with pH=0.02 to 0.56 (Varekamp et al., 2001; Pedrozo et al., 2002; Wendt-Potthoff and Koschorreck, 2002). During our March 2003 visit, the spring had a pH of 1.55 and SC= 32.3 mS/cm at 67.5 °C, with very high concentrations of SO_4^{2-} (14750 mg/L), Cl^- (9850 mg/L) and F^- (737 mg/L). Immediately after the sample cooled to ambient temperature, the pH had dropped to 1.43 and the SC had risen to 41.3 mS/cm. These changes were most likely due to dissociation of HSO_4^- ion pairs with decrease in temperature. Iron was the most abundant of the rock-forming elements (2650 mg/L), and based on Ferrozine analysis nearly all (>97%) of the dissolved iron was present in the ferrous state. Fig. 2 is a plot of the concentration of solutes in the hot-spring water normalized to their respective concentrations in global average andesite rock (<http://www.geokem.com/files/Av-Andesite2.xls>). The elements Ti, Cu, P, Si and Ba showed the lowest normalized concentrations, implying a relatively low degree of hydrothermal mobility for these elements. Silica may have precipitated during cooling of the hydrothermal solutions and is only sparingly soluble in low-pH waters, and the immobility of TiO_2 is well known. It is likely that the concentration of Ba in the thermal spring was limited by precipitation of barite. The low concentration of Cu (0.03 mg/L) rela-

tive to other trace metals (e.g., Zn=7.73 mg/L) is noteworthy, and raises the possibility that Cu may have been sequestered in the volcanic hydrothermal system, perhaps as a porphyry or “high-sulfidation” type epithermal mineral deposit.

Along its journey from the source to Lake Caviahue, discharge in the Upper Rio Agrio increased several-fold from snowmelt and influx of several minor tributary streams. At the inlet to Lake Caviahue (Site 3), the river had a pH of 2.43 and SC=5.26 mS/cm. These properties would have varied diurnally, as the discharge in the river visibly increased in the late afternoon due to snowmelt on the upper reaches of the volcano. Ferrozine analysis of a single stream sample at Site 3 indicated that ~20% of the dissolved Fe was present as Fe(III). This indicates that relatively little Fe(II) was oxidized to Fe(III) during the swift passage down the volcano. Also, based on the apparent conservative behavior of total dissolved Fe in the Upper Rio Agrio (see below), there was probably negligible precipitation of secondary ferric minerals in 2003. It is likely that a diurnal pattern in Fe(II)/Fe(III) ratio exists at Site 3, due to day-time photo-reduction of Fe(III) (McKnight et al., 1988, 2001).

Although accurate streamflow measurements were not made in our 2003 campaign, an attempt was made to assess the conservative or non-conservative behavior of solutes in the Upper Rio Agrio by normalizing each concentration to the corresponding concentration of dissolved fluoride ion (Fig. 3a, b). It was assumed that F^- itself behaved conservatively in the watershed (geochemical modeling showed that all common F-

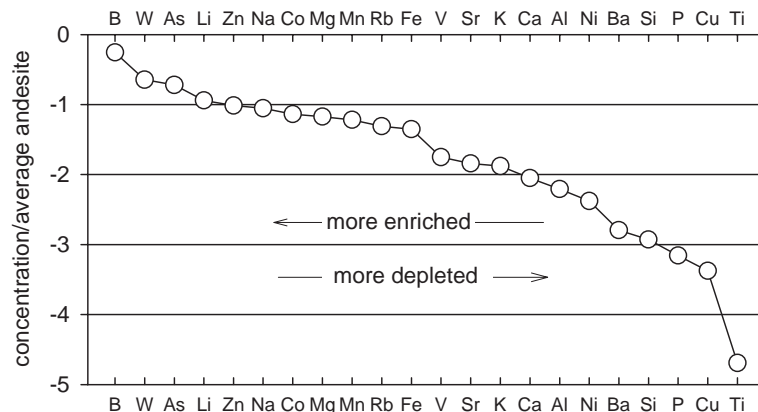


Fig. 2. Concentrations of solutes in the hot springs source of the Upper Rio Agrio, normalized to the respective concentrations in average andesite. The data are plotted in units of the logarithm of the concentration ratio.

bearing minerals, such as fluorite and fluorapatite, were strongly undersaturated in Rio Agrio water), and that snowmelt and tributary streams had negligible concentrations of F^- . Although Cl^- is more commonly used for this type of tracer analysis, the tributary streams had elevated Cl^- , which would have complicated the interpretation of the results. The F-normalized concentrations for most solutes – including the REE – remained essentially unchanged, or increased slightly between Site 1 (Agrio source) and Site 3 (inlet to Lake Caviahue), implying more or less conservative behavior in this stream reach. More substantial increases in Ca, K, and P were noted, which could be due to dissolution of primary or secondary minerals in the riverbed by the acidic waters and/or inputs from tributary streams and groundwater.

3.1.3. Lake Caviahue

Lake Caviahue is a large (surface area=9.2 km², mean depth ~50 m), glacially-carved lake with two distinct arms separated by a narrow peninsula. The

major inputs to the lake are the Upper Rio Agrio and the Rio Dulce (Site 4), the latter being a pH-neutral stream entering the lake north of the village of Caviahue (Fig. 1). Lake Caviahue also receives a large amount of runoff and overland flow during the Austral Spring due to snowmelt from the surrounding highlands. Despite being physically separated over most of their length, both arms of the lake have a very similar chemical composition (Varekamp, 2003), as shown in the vertical profiles from March 2003 (Fig. 4). The lake lacked a distinct thermocline, instead showing a gradual decrease in temperature with depth. The SC of the lake increased with depth, whereas the total dissolved solids as determined by ICP and IC analyses showed no change within the analytical error. The increase in SC is possibly explained by dissociation of HSO_4^- and/or $FeSO_4^+$ ion pairs in the colder, deeper water. The pH of the lake was nearly constant from top to bottom at 2.65 ± 0.10 , and the entire water column was oxic (dissolved oxygen >7 mg/L). The Eh of the lake was most likely controlled by Fe(II)/Fe(III) equilibria, and Ferrozine analysis of samples from the North Arm (Site 5) showed an increase in the proportion of Fe(II) towards the surface (Fig. 4). This increase in Fe(II) was possibly due to photo-reduction in the clear lake water, as the oxic conditions should have inhibited the activity of Fe-reducing bacteria in the lake.

Most major and trace elements showed no significant variation with depth in either arm of the lake (“significant” is here defined as a relative standard deviation greater than 5%). Aside from the rare earth elements (discussed below), the lone exception was P, which showed a decrease in dissolved and total concentration towards the surface of the lake (0.34 ± 0.01 below 60 m, as opposed to 0.29 ± 0.01 mg/L above 10 m). A similar decrease in soluble reactive P towards the surface of Lake Caviahue was reported by Pedrozo et al. (2001). This phenomenon may reflect uptake of P by planktonic microorganisms in the photic zone of the lake. Overall, Lake Caviahue is very highly enriched in P relative to N (our analyses gave P/N mass ratios of roughly 100), indicating that the lake is strongly N-limited in terms of its nutrient budget (Pedrozo et al., 2001).

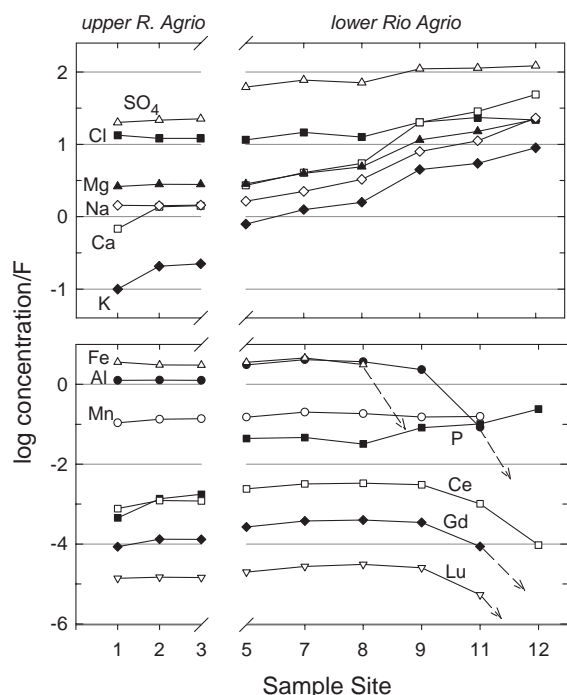


Fig. 3. Concentrations of major solutes (top) and trace solutes (bottom) in the Rio Agrio watershed, normalized to the concentration of dissolved F^- (fluoride ion). Arrows indicate that the concentration of the solute in question dropped below the analytical detection limit.

3.1.4. Lower Rio Agrio

The Lower Rio Agrio changes character dramatically between the point where it exits Lake Caviahue

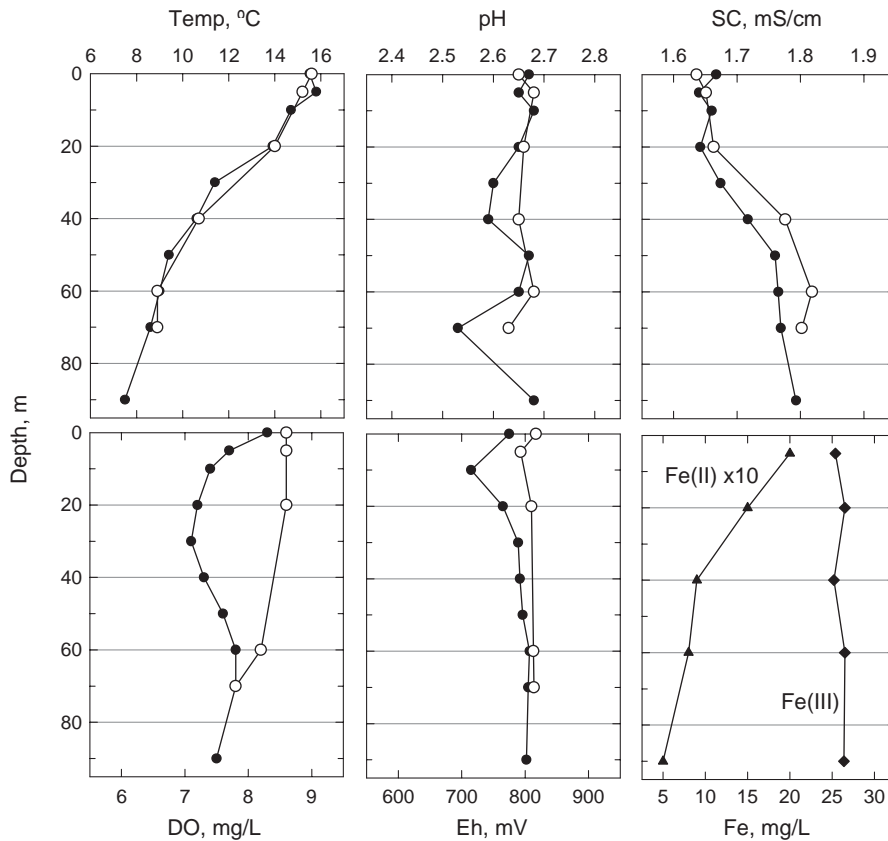


Fig. 4. Vertical profiles in pH, temperature (T), specific conductance (SC), dissolved oxygen (DO) and electrical potential (Eh) in Lake Caviahué, collected in March, 2003. The closed symbols correspond to the North Arm (Site 5), while the open symbols denote the South Arm (Site 6). The dissolved Fe speciation profile is for the North Arm only.

(Site 7) and where it passes through the city of Loncopue (Site 12), the furthest downstream point sampled. Significant tributaries include the Trolope, Norquin, and Hualcupen rivers (Fig. 1), the latter joining the R. Agrío just upstream of Loncopue. Upstream of the Rio Trolope, the riverbed was black, and showed no obvious secondary precipitates. Downstream of the Trolope, the riverbed was a vivid orange-red color, indicating the presence of secondary Fe minerals. In the mixing zone, hydrous ferric oxide (HFO) was observed to precipitate almost instantaneously in response to the increase in pH. From this point all the way to Site 9, the riverbed was stained orange-red, indicating nearly continuous precipitation and downstream advection of HFO or other ferric precipitates. In addition, ferricrete deposits (Fe-oxide cemented gravel) were noted at several localities,

especially upstream and downstream of Site 9. Below the confluence of the Rio Norquin, abundant precipitates of hydrous Al oxide (HAO) formed, as the pH of the Rio Agrío increased from 4.67 to 6.09. These precipitates imparted a turbid, milky appearance to the river at sampling Site 11. At our furthest downstream site (Loncopue) the pH of the Agrío had increased to 8.30, and the water was clear. However, the existence of red- and white-stained boulders suggests that at certain times of the year the river may run acidic as far downstream as Loncopue.

Based on visual estimates and crude streamflow calculations, the discharge of the Agrío decreased substantially between Sites 8 and 9. Subsequent reconnaissance in March 2004 showed the existence of several large irrigation diversions taking water from the main stem and heading to irrigated land to the

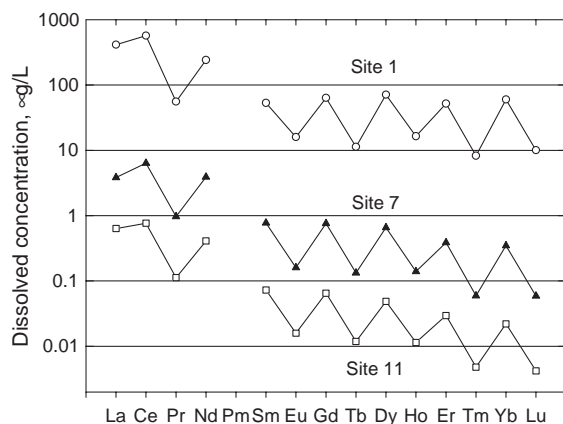


Fig. 5. Absolute concentrations of dissolved REE at the source of the Upper Agrio (Site 1), the outlet to Lake Caviahue (Site 7), and downstream of the confluence of the Rio Norquin (Site 11).

south (Fig. 1). It is somewhat remarkable that the local ranchers were using acidic water to irrigate their fields. Some of this water was observed to return to the main stem of the Lower Agrio as seeps and springs at the base of the irrigation canals. The pH of the return water was near-neutral, attesting to the ability of the alkaline soil and caliche-coated boulders underlying the ditches to neutralize the acidity of the river. Influx of neutral-pH irrigation return flow, as well as natural groundwater seepage, was most likely the main reason for the increase in pH of the Rio Agrio between Sites 8 (pH 3.19) and 9 (pH 4.67) in March 2003, as no large tributary streams exist in this portion of the watershed.

The F-normalized concentrations of all major solutes in the Lower Rio Agrio increased with distance downstream (Fig. 3), reflecting inputs from the Trolope and Norquin rivers, as well as irrigation return flow. Amongst the trace elements, only P showed a similar increase in normalized concentration with distance. Dissolved Mn showed no change in F-normalized concentration, implying conservative behavior over the entire river. Normalized Fe concentrations decreased slightly between Sites 7 and 8 (consistent with HFO deposition beyond the Trolope confluence), and then dropped below the limit of detection between Sites 8 and 9. Although some precipitation of Al occurred between Sites 8 and 9, most of the decrease in dissolved Al load occurred downstream of the confluence of the Rio Norquin, as

pH rose from 4.7 to 6.1. The REE behaved more or less conservatively in the lower river until the confluence of the Norquin (Site 10), at which point their dissolved concentrations dropped rapidly to values near the limit of analytical detection. The behavior of REE in the lower river is discussed in more detail below.

3.2. REE results

Dissolved REE concentrations measured in this study varied over 5 orders of magnitude. The absolute concentration profiles (Fig. 5) show the characteristic zig-zag pattern that is a reflection of the distribution of REE in the Earth's crust according to whether each element is odd or even-numbered. The decrease in dissolved REE concentration with distance downstream was partly due to dilution, and partly to chemical attenuation. More detailed discussions of the behavior of REE in each component of the watershed are given in the following sections.

3.2.1. Crater lake and Upper Rio Agrio

Fig. 6A shows the REE concentration patterns for water from the source of the Upper Rio Agrio (Site 1) and the Copahue crater lake. To more conveniently

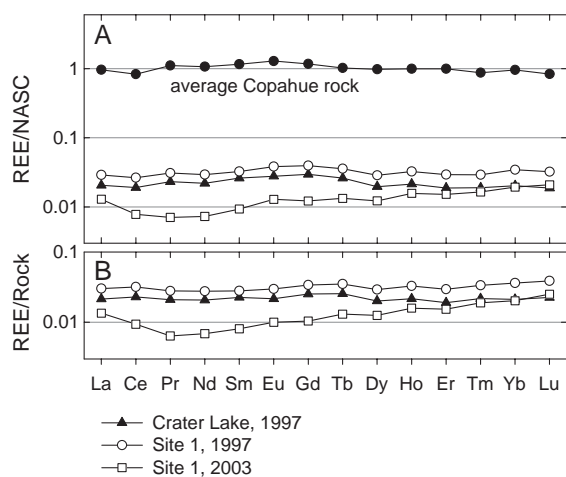


Fig. 6. Dissolved REE profiles of acidic waters in the Copahue crater lake and Rio Agrio source (Site 1), normalized to A) North American Shale Composite (NASC), and B) the average composition of a suite of andesitic rocks from Copahue Volcano. The NASC-normalized REE composition of Copahue rocks is also shown in "A".

view inter-element trends, the REE analyses have been normalized to North American Shale Composite, or NASC (Gromet et al., 1984). The results show essentially flat normalized REE profiles for the crater lake and 1997 Agrio source, indicating that the acidic waters had an REE pattern similar to that of NASC, which itself is thought to represent the average composition of the Earth's continental crust. Incompatible trace element data from the Copahue rock suite also show strong similarities with mean bulk crustal values (Goss, 2001; Varekamp et al., in press). The Agrio source in 2003 was depleted in LREE in comparison to 1997. This difference may have been caused by internal processes within the volcano itself, such as the episodic injection of fresh volcanic rock into the source area of the geothermal system. Long-term temporal shifts in the major-ion composition of the Upper Rio Agrio have been attributed to cyclic injection of fresh magma into the volcano (Varekamp et al., 2001, 2004). It is also possible that the REE are fractionated during hydrothermal water–rock interaction, and that the extent of this fractionation varies with time. Fig. 6A includes the NASC-normalized REE profile for average andesitic rock from Copahue Volcano (Appendix D). The average of 14 rock samples from Copahue is remarkably similar to NASC in both its relative and absolute REE abundance (REE/NASC ratios near 1.0). For this reason, the REE profiles of the thermal waters when normalized to average Copahue rock (Fig. 6B) are nearly identical to the NASC-normalized profiles (Fig. 6A). The depletion in LREE for the hot-springs source in 2003 implies that these elements were somehow selectively retained in the rock during hydrothermal alteration, or that they were selectively leached out of the rock by a pre-existing hydrothermal event. It is also possible that the intrusion of new magma in 2000 led to a change in the REE composition of the associated hydrothermal fluids.

3.2.2. Lake Caviahue

Shale-normalized REE profiles for the North Arm of Lake Caviahue are plotted as a function of depth in Fig. 7. The results show a weak enrichment in the middle REE (note the small range in scale of the y-axis), with a negative Dy anomaly, and a weak negative Ce anomaly. Whereas Ce anomalies are relatively common in oxidized waters (due to the unique ability of Ce to be oxidized to the tetravalent state),

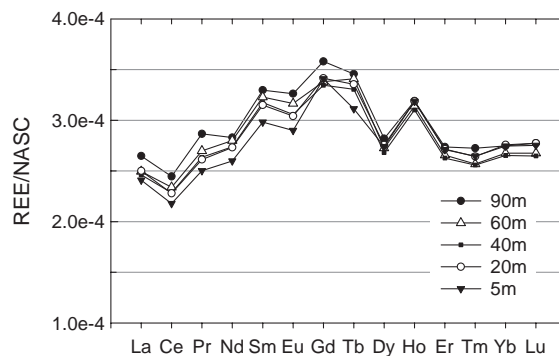


Fig. 7. NASC-normalized profiles of dissolved REE in the North Arm of Lake Caviahue, collected in March, 2003, at depths of 5, 20, 40, 60, and 90 m.

we are at a loss to explain the Dy anomaly, other than to dismiss it as an analytical artifact.

Whereas the heavy REE showed no change in dissolved concentration with depth, the light REE showed a 15–20% decrease in concentration towards the surface of the lake. A comparison of this result with the REE patterns in Fig. 6 raises the possibility that the deep lake may contain a higher percentage of older water from the Upper Rio Agrio that was less depleted in light REE (Varekamp, 2003). Another possibility is that the light REE are somehow being selectively removed in the upper portions of the lake. However, a comparison of filtered and non-filtered samples showed no difference in REE concentration, indicating that the REE were not partitioning to any discernable extent into suspended particles at this time.

Fig. 3 shows an increase in F-normalized REE concentrations between the Upper Rio Agrio (Site 3) and the North Arm of Lake Caviahue (Site 5), as well as the Lower Rio Agrio near the outlet to the lake (Site 7). Several other element ratios show similar increases (e.g., Al/F is 1.3 in the Upper Rio Agrio and 3.1 in Lake Caviahue). This is because the composition of Lake Caviahue, with an estimated residence time of 3–4 years (Varekamp, 2003), integrates the chemistry of its influent waters over a several year period. In the year following the 2000 eruption of Copahue, much higher rock-derived element fluxes were noted in the Upper Rio Agrio (Varekamp et al., in press). Thus, the increase in F-normalized REE concentrations does not mean that a chemical reaction occurred in the lake (such as precipitation of an F-bearing mineral, or influx of REE from an unknown source). Since evapoconcentra-

tion would have increased the concentration of both F and REE, this process cannot explain the change in the ratio of these solutes.

3.2.3. Lower Rio Agrio

The concentration of REE in the Lower Rio Agrio decreased substantially between the outlet of Lake Caviahue and Loncopue (Fig. 5). Fig. 3 suggests that most of the decrease between Sites 7 and 9 was simply due to dilution. However, downstream of the confluence of the Rio Norquin, the dissolved concentrations of REE decreased much more than simple dilution can account for (Fig. 3). Based on a comparison of filtered and non-filtered concentrations, the percentage of total REE transported as suspended particles increased dramatically below the Rio Norquin (Fig. 9). The light REE (La, Ce) partitioned to a lesser extent into the solid phase at Site 11 than did the

middle and heavy REE. Possible mechanisms for this REE attenuation include adsorption onto HAO and HFO particles, and precipitation of insoluble REE minerals. This is discussed in more detail below.

In addition to the decrease in REE concentration with distance downstream, there was also a subtle but systematic change in the slope of the NASC-normalized REE profiles. Overall, the upper river had REE patterns with a positive slope across the lanthanide series, whereas a slight negative slope developed in its lower reaches (Fig. 8A). The shift in slope in the lower river was most likely due to selective partitioning of heavier REE into suspended particles or secondary minerals and biofilms on the streambed. These results complement those of REE patterns for suspended particles shown in Fig. 9. Besides the overall change in slope, the negative Ce and Dy anomalies increased slightly in magnitude with distance downstream (Fig.

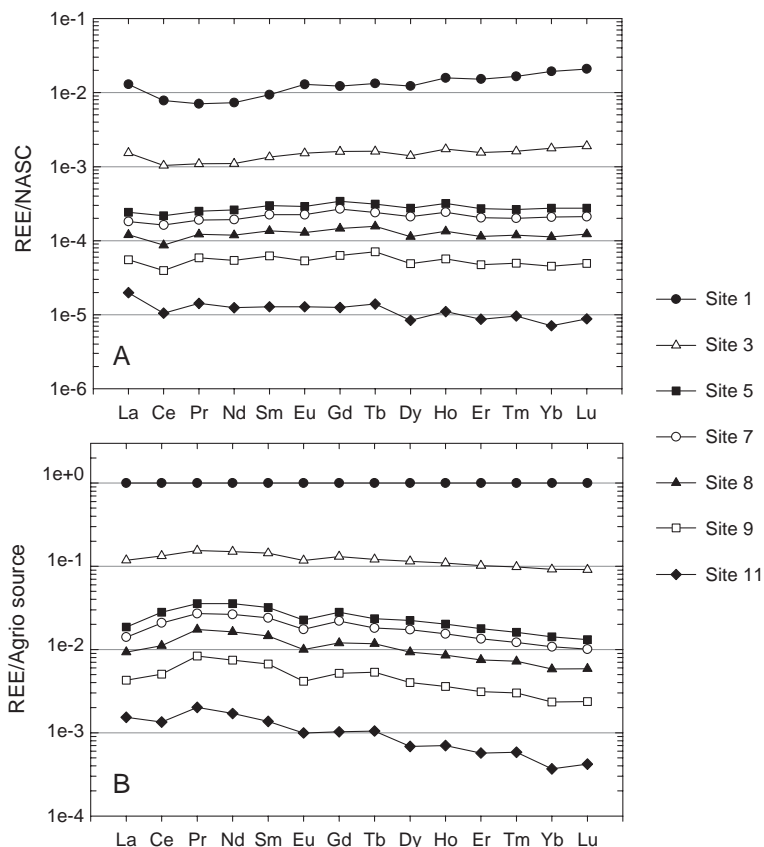


Fig. 8. Comparison of normalized dissolved REE profiles at selected sites in the Upper and Lower Rio Agrio: A) REE concentrations normalized to NASC; B) REE concentrations normalized to the Rio Agrio source (Site 1).

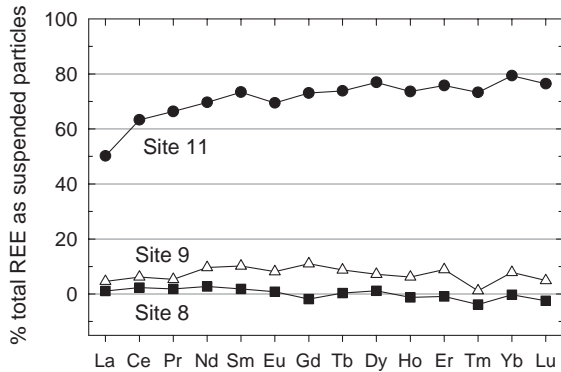


Fig. 9. The percentage of total REE in the Lower Rio Agrio as suspended particles at sample Sites 8, 9, and 11.

8A). The downstream trends in REE profiles were re-examined by normalizing the dissolved REE concentrations to Site 1, the hot-spring source of the Rio Agrio. When this was done (Fig. 8B), the Dy and Ce anomalies were less apparent, and a slight negative Eu anomaly appeared. It is important to note that the

magnitude of all of these anomalies is rather small, and could be explained in part by analytical error.

4. Discussion

4.1. Saturation indices of Fe and Al solids

Based on Visual MINTEQ calculations (Fig. 10), the Upper Rio Agrio was undersaturated with all Al-bearing solids, but was supersaturated with jarosite (including Na, K, and H_3O^+ varieties), and close to equilibrium with strengite ($\text{FePO}_4 \cdot \text{H}_2\text{O}$) and goethite. It is likely that jarosite was present in the sediment of the upper river, but was not precipitating quickly enough to buffer the dissolved Fe^{3+} concentrations to equilibrium levels. Because the rate of precipitation of jarosite is very slow, supersaturation with this phase is common in Fe-rich waters (Bigham and Nordstrom, 2000). Likewise, direct precipitation of goethite is kinetically inhibited, although the fact that the satura-

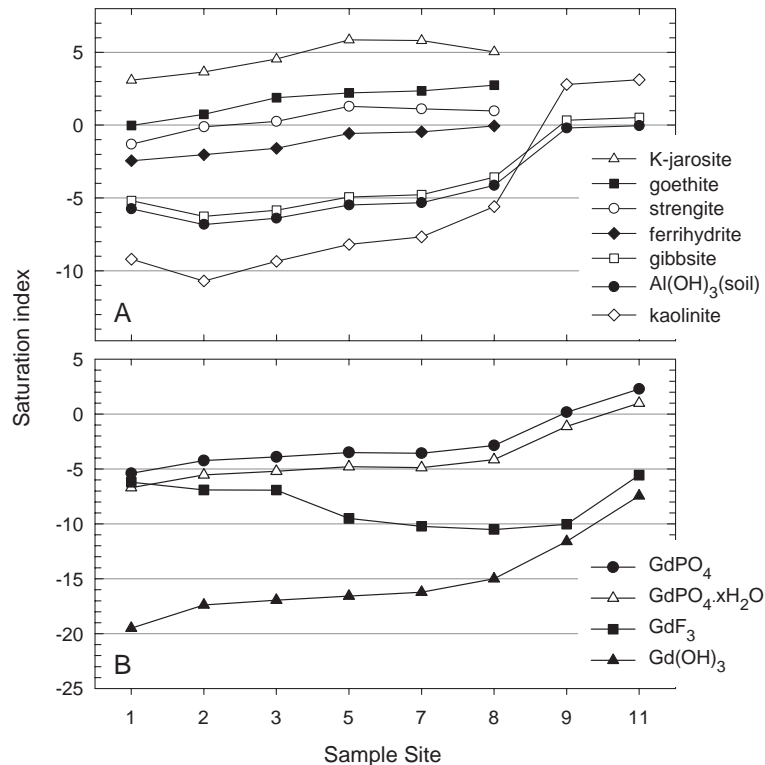


Fig. 10. Changes in the saturation index of selected Fe and Al solids (A) and Gd solids (B) with distance downstream in the Rio Agrio watershed. Saturation indices for Fe minerals could not be evaluated beyond Site 8 because dissolved Fe concentrations were below detection.

tion index ($\log Q/K$) of this phase was very close to zero for the hot springs source (Site 1) suggests that the acidic thermal water may have equilibrated with goethite (or hematite) on route to the surface of the volcano. Strengite was slightly to moderately supersaturated for all samples in the Upper Rio Agrio where ferric iron was detected (Fig. 10). It is plausible that precipitation of strengite placed an upper limit on the concentration of soluble orthophosphate in the Rio Agrio, as well as Lake Caviahue.

Downstream of Lake Caviahue, the saturation indices of ferrihydrite (i.e., hydrous ferric oxide, or HFO) increased in a manner that agreed with visual observations. Ferrihydrite was predicted to precipitate beyond the Rio Trolope, as the saturation index was very close to zero at Site 8 (Fig. 10). This is consistent with the abundance of bright orange-red precipitates in the R. Agrio below the R. Trolope, but not upstream of this tributary. Beyond Site 8, the concentration of dissolved ferric iron was

below detection. However, the persistence of orange-red precipitates on the river boulders suggests that the river was most likely in a state of near-equilibrium with ferrihydrite (or HFO) over its lower reaches. A number of aluminous phases were close to equilibrium in the Lower R. Agrio at Sites 9 and 10 (Fig. 10). Phases with saturation indices near 0 included gibbsite, poorly crystalline $\text{Al}(\text{OH})_3$, and imogolite (hydrous Al-silicate). Based on the rapid rate of Al precipitation at the confluence of the R. Norquin (as evidenced by a white turbidity downstream of the mixing zone), the phase most likely controlling dissolved Al levels would have been poorly crystalline $\text{Al}(\text{OH})_3$ (i.e., hydrous Al oxide, or HAO).

4.2. Aqueous speciation and saturation indices of REE

At the mouth of the Upper Rio Agrio (Site 3), MINTEQ calculations predict that the dominant aque-

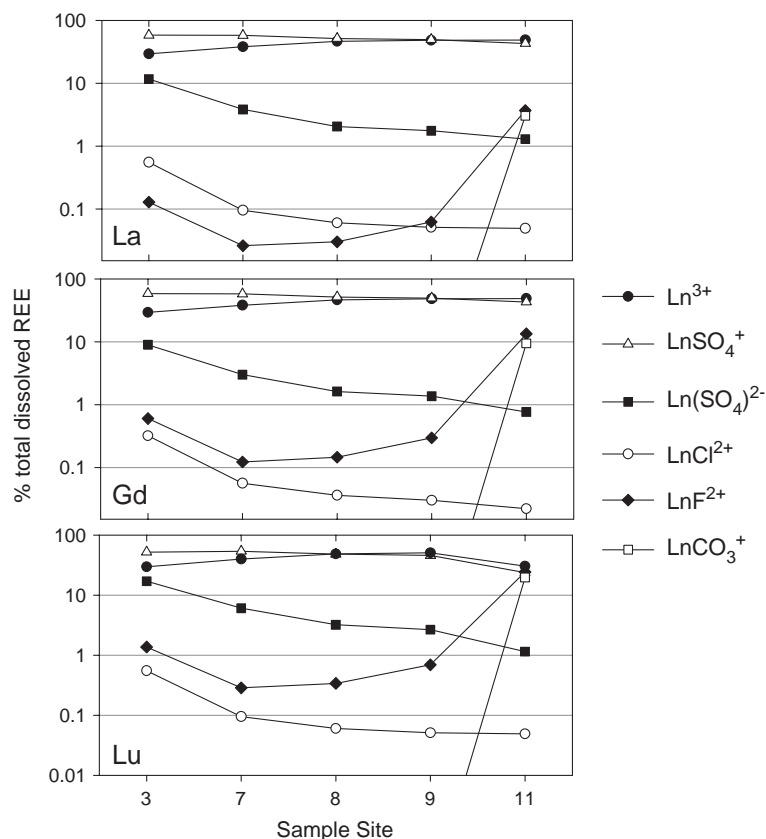


Fig. 11. Changes in aqueous speciation of La, Gd, and Lu with distance downstream in the Rio Agrio watershed.

ous REE species were Ln^{3+} , LnSO_4^+ , and $\text{Ln}(\text{SO}_4)_2^-$ (Fig. 11). (Here, Ln refers to any lanthanide element.) With distance downstream, the 1:2 sulfate ion pairs were predicted to be less significant whereas the relative abundance of the uncomplexed Ln^{3+} ions increased. Despite the very high F concentrations in the upper river, fluoride complexes of REE were insignificant until the pH had risen above 6, downstream of the Norquin confluence. This is because >98% of the total dissolved F in solution was calculated to be complexed with aqueous Al in the upstream waters (see also Gimeno et al., 2000). Only when the Al precipitated out as HAO downstream of the Rio Norquin did concentrations of free F^- become substantial enough to contribute to REE complexation. In addition, the 1:1 carbonate complex became significant at Site 11, due to the rise in pH from the addition of bicarbonate alkalinity from the Rio Norquin. Complexation with F^- and CO_3^{2-} was strongest for Lu and least strong for La (Fig. 11), underscoring the general trend of increasing stability of complexes with these ligands across the lanthanide series.

The saturation indices for all common REE solids were strongly negative until Site 9, just upstream of the confluence with the Norquin River (Fig. 10b). At Site 9, some of the more abundant REE (such as La, Ce, Nd, Gd) were approaching saturation with LnPO_4 (where Ln=any trivalent lanthanide). Solubility products for the LnPO_4 phases in the Visual MINTEQ database were taken from Liu and Byrne (1997). At Site 11, all of the REE were strongly supersaturated with LnPO_4 , as well as its hydrous variety ($\text{LnPO}_4 \cdot x\text{H}_2\text{O}$). This raises the possibility that the aforementioned attenuation of dissolved REE in the mixing zone of the Agrio and Norquin rivers could be due to precipitation of REE-phosphate compounds, as has been documented elsewhere (Byrne and Kim, 1993; Sholkovitz, 1995). However, a more detailed examination of inter-element trends suggests that this may not be the case. Fig. 12 shows the calculated saturation index for each LnPO_4 compound, assuming pure end members. The results exhibit a complex zig-zag pattern (which is due to the variation in natural abundance of odd vs. even-numbered elements) that slopes steeply from left to right across the lanthanide series. This indicates that the heavy REE were less supersaturated with respect to LnPO_4 , and therefore would have had a weaker tendency to partition into

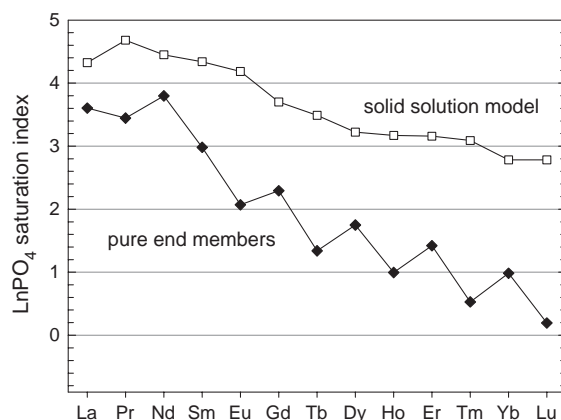


Fig. 12. Inter-element changes in the saturation index of LnPO_4 compounds in the Rio Agrio at Site 11 (below confluence of Rio Norquin). The calculations assume either a pure end member model (A), or an ideal solid solution model (B).

the solid phase. This is the *opposite* pattern to what was observed at Site 11, where the heavy REE were found to partition to a greater degree into suspended particles relative to the light REE (Fig. 8). The calculations were refined by incorporating a solid solution model. The mole fraction of each LnPO_4 component in the solid solution was calculated from the observed decrease in aqueous concentration of each element between Sites 9 and 11, and assuming that this decrease was only due to precipitation of LnPO_4 . The computed saturation indices assuming the solid solution model show a smoother pattern across the lanthanide series (Fig. 12), but are still sloped downwards. These observations are fairly strong evidence against the hypothesis that REE fractionation trends observed in the Lower Rio Agrio were due to precipitation of LnPO_4 compounds. Whereas precipitation of LnPO_4 may have occurred to some extent, another mechanism is needed to explain the observed REE fractionation patterns.

4.3. Adsorption of REE

In the absence of strong evidence for precipitation of REE solids, the most likely alternate hypothesis to explain the sharp decrease in dissolved REE load beyond the Rio Norquin confluence is adsorption onto hydrous oxides of Fe and/or Al. Previous studies of REE in streams impacted by acid mine drainage have shown that the REE tend to behave conservatively up to

a pH of roughly 5.5, above which point they begin to partition strongly onto suspended particles of hydrous metal oxide (Verplanck et al., 2004; Gammons et al., in press; Wood et al., in press). The pH-dependence of solid-aqueous partitioning of REE appears to be controlled by an adsorption edge of aqueous lanthanide ions onto HFO and HAO surfaces, which presumably occurs near pH 5.2 to 5.5 (Bau, 1999; Coppin et al., 2002; Verplanck et al., 2004). Furthermore, both Verplanck et al. (2004) and Gammons et al. (in press) illustrated that the light REE partitioned to a lesser extent into the suspended solids than did the middle and heavy REE. This behavior is similar to what was observed in the Rio Agrio at Site 11, and also to the experimental studies of Bau (1999) and Ohta and Kawabe (2001), but is opposite to the trend in REE partitioning that is typically observed in waters of higher alkalinity, such as seawater (Koeppenkastrup and De Carlo, 1992). Whereas Verplanck et al. (2004) concluded that the REE were primarily sorbing onto fresh HFO surfaces in the stream that they investigated (Uncle Sam Gulch, Montana, USA), in the case of the Lower Rio Agrio it is more likely that the REE adsorbed onto hydrous Al particles. The suspended solids at Site 11 were dominated by HAO as opposed to HFO, as most of the dissolved Fe had already deposited many km upstream between Sites 8 and 9. The Al/Fe mass ratio in suspended solids at Site 11 was >18:1, and the mole ratio was >37:1 (these ratios are minimum values, because the concentration of suspended Fe at Site 11 was below the detection limit of 0.1 mg/L). Also, based on the data in Appendix A, the suspended sediment contained insignificant concentrations of Na, K, Ca, or Mg, indicating that these cations were scarcely present in the HAO particles. This rules out the possibility that smectite or illite could have been the dominant suspended material.

A number of previous workers have documented the adsorption of REE onto clay minerals such as kaolinite and smectite (Coppin et al., 2002, and references therein). For example, Maza-Rodriguez et al. (1992) found that the heavy REE were more strongly sorbed onto montmorillonite than the light REE, which is consistent with the pattern displayed in the Lower Rio Agrio. However, we are not aware of a laboratory study addressing sorption of REE onto rapidly precipitated HAO. Gammons et al. (in press) concluded that REE attenuation in Fisher Creek (a mountain stream with a

steep pH gradient in Montana, USA) was caused by adsorption onto actively forming HFO and HAO. The adsorption reaction was favored by increase in water temperature, resulting in strong diel variations in the degree of partitioning of REE between suspended solids and aqueous solution in the lower, pH-neutral reach of Fisher Creek (Gammons et al., in press). Such behavior was also documented in the Rio Agrio by our group during a follow-up field study in March of 2004 (Parker and Gammons, 2004; Wood et al., in press).

5. Conclusions

This study has documented changes in the concentration of major ions and rare earth elements in a mountain watershed in Patagonia that changes pH from hyperacidic (<2) to near-neutral over a distance of >40 km. The overall trends in Fe, Al, and other rock-forming elements followed predicted patterns, with precipitation of Fe occurring in the pH range 2.5 to 4, and precipitation of Al in the pH range 4.5 to 6. A comparison of REE profiles at the hot-spring source of the Rio Agrio in 1997 and 2003 showed distinct changes with time, perhaps related to the episodic injection of fresh volcanic rock into the source area of the geothermal system. The chemical evolution of the hydrothermal system is also evident from the higher F-normalized REE and major element concentrations in Lake Caviahue waters as compared to the Upper Rio Agrio in 2003.

Once discharged to the surface, the rare earth elements (REE) were conservative through the watershed until the confluence of a tributary raised the pH of the Rio Agrio above 6.0. Downstream of this point, the dissolved concentrations of REE dropped sharply, and the REE partitioned into suspended particles. The dominant REE attenuation mechanism is believed to have been adsorbed onto freshly precipitated hydrous aluminum oxide (HAO), with the light REE being less strongly adsorbed than the middle and heavy REE. This general pattern of selective adsorption of heavier REE caused a subtle shift in the shape of NASC-normalized REE profiles from being slightly positive in the Upper Rio Agrio, to being slightly negative in the Lower Rio Agrio. A weak negative Ce anomaly was noted in many samples, becoming stronger in the lower reaches of the river.

The results of this study are in broad agreement with previous investigations of REE transport in acidic, mining-impacted streams (e.g., Verplanck et al., 2004; Gammons et al., in press). However, unlike the study of Verplanck et al. (2004), which concluded that hydrous ferric oxide (HFO) was the dominant substrate for REE adsorption at pH > 5, in the case of the Rio Agrio it is clear that HAO played a more important role than HFO. This may not reflect a particular chemical affinity of REE for Al, but rather may be a result of the fact that the precipitation of HAO in the Rio Agrio happened to occur over the same pH range as the adsorption edge for lanthanide ions onto hydrous metal oxide surfaces. Additional research on the sorption of REE onto HAO is recommended, especially with regards to the origin of inter-element fractionation

patterns, how temperature and pH may affect REE partition coefficients, and the competitive sorption of REE onto mixtures of HAO and HFO.

Acknowledgments

We thank Guadalupe Beamud and José M. De Giusto for their assistance in collecting samples in Cavihue, and two anonymous reviewers for helpful suggestions. Funding for travel was provided in part from an International Exchange grant to Montana Tech from the U.S. Department of State (CHG) and from ANPCyT-PICT01-08186 (FLP). Funding for the research of J.C. Varekamp was provided by grants from NSF (#INT-9704200 and #INT-9813912) and by the National Geographic Society (Grant #7409-03). [LW]

Appendix A. Concentration (mg/L) of selected metals in the Rio Agrio watershed

Site	Al	As	Ba	Ca	Fe	K	Mg	Mn	Na	P	Si	Rb	Sr	Zn
<i>Dissolved metal concentration (0.45 µm filtration)</i>														
1	921	4.78	0.58	503	2650	73.6	1930	79.8	1060	0.33	90.2	1.72	5.84	7.73
2	86.1	0.34	0.06	93.3	208	14.1	191	9.03	97	0.09	25.2	0.15	0.82	0.59
3	79.1	0.29	0.07	89.2	191	14.1	176	8.63	91	0.11	25.4	0.16	0.77	0.53
4	ND	ND	0.06	15.6	ND	3.57	12.8	0.20	9.8	0.07	12.3	0.10	0.08	ND
5*	20.2	0.01	0.06	17.9	23.4	5.21	18.7	0.99	10.8	0.29	12.3	0.10	0.16	0.03
6*	20.2	ND	0.06	17.5	22.7	5.29	17.9	0.96	10.6	0.29	12.3	0.10	0.16	0.03
7	15.2	0.01	0.06	15.0	16.8	4.64	14.7	0.74	8.3	0.17	12.9	0.09	0.13	(1.16)
8	6.99	ND	0.05	10.4	6.0	3.01	9.3	0.35	6.3	0.06	9.6	0.09	0.09	ND
9	2.19	ND	0.06	18.9	ND	4.22	10.8	0.14	7.5	0.08	19.2	0.11	0.15	ND
10	ND	ND	0.05	27.1	ND	2.60	11.0	ND	12.3	0.13	19.2	0.09	0.13	ND
11	0.06	ND	0.06	21.4	ND	4.08	11.3	0.12	8.4	0.08	19.4	0.09	0.15	ND
12	ND	ND	0.06	15.6	ND	2.87	7.1	0.00	7.4	0.08	15.5	0.09	0.11	ND
<i>Total metal concentration (unfiltered)</i>														
1	930	4.76	0.58	508	2670	73.5	1950	80.6	1080	0.09	95.1	1.71	5.93	7.52
2	86.2	0.34	0.10	93.9	210	14.4	189	8.96	96	0.14	26.4	0.15	0.83	0.56
3	79.5	0.31	0.09	89.1	192	13.9	176	8.64	89	0.14	26.2	0.16	0.78	0.51
4	0.01	ND	0.06	15.6	ND	3.64	12.8	0.21	10	0.06	12.3	0.10	0.08	ND
5*	20.4	0.01	0.06	18.0	23.6	5.22	18.8	1.00	11	0.26	12.5	0.10	0.16	0.03
6*	20.1	0.01	0.06	17.4	22.6	5.37	17.8	0.95	10	0.31	12.2	0.10	0.16	0.04
7	14.8	0.00	0.06	14.6	16.6	4.44	14.4	0.72	9.0	0.23	12.5	0.09	0.12	0.01
8	6.99	ND	0.05	10.3	6.5	3.03	9.2	0.35	6.1	0.14	9.65	0.10	0.09	ND
9	2.59	ND	0.06	18.8	ND	4.22	10.7	0.14	7.4	0.06	19.2	0.11	0.15	ND
10	0.27	ND	0.05	27.6	ND	2.64	11.3	0.01	12	0.16	20.0	0.08	0.13	ND
11	1.85	ND	0.06	21.6	ND	4.13	11.3	0.12	8.4	0.05	20.3	0.09	0.15	ND
12	0.19	ND	0.05	16.0	ND	2.98	7.3	0.01	7.7	0.07	16.2	0.09	0.11	ND
B1	0.01	ND	0.05	0.52	ND	ND	1.2	ND	0.3	0.05	ND	0.07	ND	ND
B2	ND	ND	0.05	0.52	ND	ND	1.2	ND	0.3	0.05	ND	0.07	ND	ND

B1 and B2 were unfiltered field blanks. ND=non-detected.

*Collected from 5 m below surface of Lake Cavihue.

Appendix B. Concentration ($\mu\text{g/L}$) of REE in Rio Agrio and tributaries

Site	La	Ce	Pr	Nd	Sm	Eu	Gd	Tb	Dy	Ho	Er	Tm	Yb	Lu
<i>Dissolved REE concentration (0.45 μm filtration)</i>														
1	410	570	56	240	53	16	64	11	71	16	52	8.2	60	10
2	54	84	9.5	40	8.4	2.0	9.0	1.5	8.8	2.0	5.7	0.88	6.0	1.0
3	49	76	8.6	36	7.6	1.9	8.3	1.4	8.1	1.8	5.3	0.81	5.5	0.91
4	0.16	0.095	0.022	0.090	0.023	0.007	0.018	0.004	0.014	0.004	0.009	0.002	0.007	0.002
7	5.8	12	1.5	6.4	1.3	0.28	1.4	0.20	1.2	0.25	0.69	0.10	0.65	0.10
8	3.8	6.3	0.97	3.9	0.77	0.16	0.76	0.13	0.66	0.14	0.39	0.059	0.35	0.059
9	1.8	2.9	0.46	1.8	0.36	0.066	0.33	0.060	0.28	0.059	0.16	0.025	0.14	0.024
10	0.013	0.018	0.006	0.026	0.019	0.006	0.009	0.002	0.009	0.002	0.006	0.002	0.006	0.002
11	0.63	0.77	0.11	0.41	0.073	0.016	0.065	0.012	0.049	0.011	0.030	0.005	0.022	0.004
12	0.023	0.030	0.008	0.034	0.019	0.007	0.011	0.003	0.011	0.003	0.008	0.002	0.006	0.002
<i>Total REE concentration (unfiltered)</i>														
1	410	560	55	240	52	16	64	11	72	16	52	8.4	61	10
2	55	84	9.5	40	8.4	2.1	9.0	1.5	8.8	1.9	5.7	0.89	6.1	1.0
3	50	77	8.7	37	7.9	1.9	8.3	1.4	8.1	1.8	5.2	0.82	5.5	0.91
4	0.22	0.14	0.032	0.11	0.028	0.008	0.027	0.005	0.019	0.005	0.011	0.002	0.009	0.002
7	5.8	12	1.5	6.4	1.3	0.27	1.3	0.20	1.2	0.24	0.66	0.096	0.62	0.097
8	3.9	6.5	0.98	4.0	0.79	0.16	0.75	0.13	0.67	0.14	0.38	0.057	0.35	0.057
9	1.8	3.1	0.49	2.0	0.40	0.072	0.37	0.066	0.31	0.063	0.18	0.025	0.15	0.025
10	0.20	0.48	0.069	0.28	0.078	0.021	0.062	0.013	0.057	0.012	0.033	0.006	0.030	0.006
11	1.3	2.1	0.33	1.35	0.27	0.052	0.24	0.045	0.21	0.043	0.12	0.018	0.11	0.018
12	0.16	0.27	0.049	0.18	0.056	0.012	0.040	0.009	0.036	0.008	0.021	0.004	0.021	0.004
B1	0.005	0.004	0.025	0.032	0.015	0.005	0.007	0.002	0.007	0.003	0.005	0.002	0.005	0.002
B2	0.004	0.004	0.005	0.012	0.015	0.005	0.007	0.002	0.007	0.002	0.005	0.002	0.005	0.002

B1 and B2 were unfiltered field blanks.

Appendix C. Concentration ($\mu\text{g/L}$) of REE in Lake Caviahue

Site	La	Ce	Pr	Nd	Sm	Eu	Gd	Tb	Dy	Ho	Er	Tm	Yb	Lu
<i>Dissolved REE concentration (0.45 μm filtration)</i>														
N05	7.7	16	2.0	8.6	1.7	0.36	1.8	0.26	1.6	0.33	0.92	0.13	0.85	0.13
N20	8.0	17	2.1	9.0	1.8	0.38	1.8	0.28	1.6	0.33	0.92	0.13	0.85	0.13
N40	7.9	17	2.1	9.0	1.8	0.38	1.7	0.28	1.6	0.32	0.89	0.13	0.82	0.13
N60	8.0	17	2.1	9.2	1.8	0.39	1.8	0.29	1.6	0.33	0.90	0.13	0.83	0.13
N90	8.5	18	2.3	9.3	1.9	0.41	1.9	0.29	1.6	0.33	0.93	0.14	0.85	0.13
S05	8.5	18	2.3	9.3	1.9	0.41	1.8	0.30	1.6	0.32	0.92	0.13	0.85	0.13
S40	8.6	18	2.3	9.7	1.9	0.42	1.8	0.30	1.6	0.32	0.92	0.13	0.84	0.13
S70	8.6	18	2.3	9.7	1.9	0.42	1.8	0.30	1.6	0.32	0.91	0.13	0.83	0.13
<i>Total REE concentration (unfiltered)</i>														
N05	7.8	16	2.0	8.7	1.7	0.37	1.8	0.27	1.6	0.33	0.90	0.13	0.84	0.13
N20	8.1	17	2.1	9.1	1.8	0.38	1.8	0.29	1.6	0.33	0.93	0.13	0.85	0.13
N40	7.9	17	2.1	9.1	1.8	0.38	1.7	0.28	1.6	0.32	0.89	0.13	0.82	0.13
N60	8.0	17	2.1	9.3	1.8	0.39	1.8	0.29	1.6	0.32	0.90	0.13	0.83	0.13
N90	8.5	18	2.3	9.5	1.9	0.41	1.8	0.30	1.6	0.33	0.93	0.13	0.85	0.13
S05	8.5	18	2.2	9.5	1.9	0.41	1.8	0.30	1.6	0.32	0.92	0.13	0.84	0.13
S40	8.6	18	2.3	9.7	1.9	0.42	1.8	0.30	1.6	0.32	0.90	0.13	0.83	0.13
S70	8.6	18	2.3	9.7	1.9	0.42	1.8	0.30	1.6	0.32	0.90	0.13	0.83	0.13

In the Site column, N= North Arm, S=South Arm, and the number is the depth (m) at which the sample was taken.

Appendix D. Concentration ($\mu\text{g/L}$) of REE in Copahue crater lake (C.L.) and the hot-springs source of the Rio Agrio (Site 1) in March 1997, and representative REE analyses (mg/kg) of rock samples from Copahue volcano

Site	La	Ce	Pr	Nd	Sm	Eu	Gd	Tb	Dy	Ho	Er	Tm	Yb	Lu
<i>Dissolved REE concentration (0.45 μm filtration, $\mu\text{g/L}$)</i>														
C.L.	660	1400	180	720	150	34	150	22	110	22	64	9.5	63	9.0
1	930	1900	240	970	180	47	210	30	170	34	100	15	110	15
<i>REE concentration (mg/L) in Copahue rock</i>														
a	44	63	8.9	37	7.4	1.7	7.0	1.0	8.7	1.1	3.7	0.5	3.4	0.4
b	29	57	8.3	34	6.2	1.6	5.6	0.8	5.5	1.0	3.6	0.4	3.0	0.4
c	15	26	3.4	13	2.3	0.4	2.2	0.3	1.9	0.4	1.4	0.2	1.0	0.2
Avg	31	61	8.7	35	6.6	1.6	6.1	0.9	5.7	1.0	3.4	0.4	3.0	0.40

a=sample 1-251199; b=sample 1-020800a; c=sample 1-170700; avg=average of 14 rock samples. All rock data from Goss (2001).

References

- Allison, J.D., Brown, D.S., Novo-Gradac, K.J., 1991. MINTEQA2/PRODEFA2, A Geochemical Assessment Model for Environmental Systems: version 3.0 Users Manual. Environ. Res. Lab., U.S. Environmental Protection Agency.
- Åström, M., 2001. Abundance and fractionation patterns of rare earth elements in streams affected by acid sulphate soils. *Chem. Geol.* 175, 249–258.
- Bau, M., 1999. Scavenging of dissolved yttrium and rare earths by precipitating iron oxyhydroxide; experimental evidence for Ce oxidation, Y-Ho fractionation, and lanthanide tetrad effect. *Geochim. Cosmochim. Acta* 63, 67–77.
- Bigham, J.M., Nordstrom, D.K., 2000. Iron and aluminum hydroxysulfates from acid sulfate waters. *Miner. Soc. Am., Rev. Mineral. Geochem.* 40, 351–403.
- Bozau, E., Leblanc, M., Seidel, J.L., Stärk, H.-J., 2004. Light rare earth elements enrichment in an acidic mine lake (Lusatia, Germany). *Appl. Geochem.* 19, 261–271.
- Byrne, R.H., Kim, K.H., 1993. Rare earth precipitation and coprecipitation behavior: the limiting role of PO_4^{3-} on dissolved rare earth concentrations in seawater. *Geochim. Cosmochim. Acta* 57, 519–526.
- Coppin, F., Berger, G., Bauer, A., Castet, S., Loubet, M., 2002. Sorption of lanthanides on smectite and kaolinite. *Chem. Geol.* 182, 57–68.
- Elbaz-Poulichet, F., Dupuy, C., 1999. Behavior of rare earth elements at the freshwater–seawater interface of two acid mine rivers: the Tinto and Odiel (Andalusia, Spain). *Appl. Geochem.* 14, 1063–1072.
- Gammons, C.H., Wood, S.A., Jonas, J.P., Madison, J.P., 2003. Geochemistry of rare earth elements and uranium in the acidic Berkeley Pit lake, Butte, Montana. *Chem. Geol.* 198, 269–288.
- Gammons, C.H., Wood, S.A., Nimick, D.A., in press. Diel behavior of rare earth elements in a mountain stream with acidic to neutral pH. *Geochim. Cosmochim. Acta*.
- Gimeno, M.J., Auqué, L.F., Nordstrom, D.K., 2000. REE speciation in low-temperature acidic waters and the competitive effects of aluminum. *Chem. Geol.* 165, 167–180.
- Goss, A.R., 2001. Magmatic evolution of Volcan Copahue, Neuquen, Argentina. B.S. thesis, Wesleyan University, Middletown, CT., 209 pp.
- Gromet, L.P., Dymek, R.F., Haskin, L.A., Korotev, R.L., 1984. The “North American shale composite”; its compilation, major and trace element characteristics. *Geochim. Cosmochim. Acta* 48, 2469–2482.
- Johannesson, K.H., Lyons, W.B., 1995. Rare-earth element geochemistry of Colour Lake, an acidic freshwater lake on Axel Heiberg Island, Northwest Territories, Canada. *Chem. Geol.* 119, 209–223.
- Johannesson, K.H., Zhou, X., 1999. Origin of middle rare earth element enrichments in acid waters of a Canadian High Arctic lake. *Geochim. Cosmochim. Acta* 63, 153–165.
- Johannesson, K.H., Lyons, W.B., Yelken, M.A., Gaudette, H.E., Stetzenbach, K.J., 1996. Geochemistry of rare earth elements in hypersaline and dilute acidic natural terrestrial waters: complexation behavior and middle rare-earth element enrichments. *Chem. Geol.* 133, 125–144.
- Kikawada, Y., Oi, T., Honda, T., Osaka, T., Kakihana, H., 1993. Lanthanoid abundances of acidic hot spring and crater lake waters in the Kusatsu-Shirane volcano region, Japan. *Geochem. J.* 27, 19–33.
- Klungness, G.D., Byrne, R.H., 2000. Comparative hydrolysis of the rare earth elements and yttrium: the influence of temperature and ionic strength. *Polyhedron* 19, 99–107.
- Koepfenkastro, D., De Carlo, E.H., 1992. Sorption of rare-earth elements from seawater onto synthetic mineral particles: An experimental approach. *Chem. Geol.* 95, 251–263.
- Lewis, A.J., Palmer, M.R., Sturchio, N.C., Kemp, A.J., 1997. The rare earth element geochemistry of acid-sulphate and acid-sulphate-chloride geothermal systems from Yellowstone National Park, Wyoming, USA. *Geochim. Cosmochim. Acta* 61, 695–706.

- Leybourne, M.I., Goodfellow, W.D., Boyle, D.R., Hall, G.M., 2000. Rapid development of negative Ce anomalies in surface waters and contrasting REE patterns in groundwaters associated with Zn–Pb massive sulphide deposits. *Appl. Geochem.* 15, 695–723.
- Liu, X., Byrne, R.H., 1997. Rare earth and yttrium phosphate solubilities in aqueous solution. *Geochim. Cosmochim. Acta* 61, 1625–1633.
- Liu, X., Byrne, R.H., 1998. Comprehensive investigation of yttrium and rare earth element complexation by carbonate ions using ICP-MS spectrometry. *J. Solution Chem.* 27, 803–815.
- Maza-Rodríguez, J., Olivera-Pastor, P., Bruque, S., Jiménez-Lopez, A., 1992. Exchange selectivity of lanthanide ions in montmorillonite. *Clay Miner.* 27, 81–89.
- McKnight, D.M., Kimball, B.A., Bencala, K.E., 1988. Iron photoreduction and oxidation in an acidic mountain stream. *Science* 240, 637–640.
- McKnight, D.M., Kimball, B.A., Runkel, R.L., 2001. pH dependence of iron photoreduction in a rocky mountain stream affected by acid mine drainage. *Hydrol. Process.* 15, 1979–1992.
- Ohta, A., Kawabe, I., 2001. REE(III) adsorption onto Mn dioxide (δ -MnO₂) and Fe oxyhydroxide: Ce(III) oxidation by δ -MnO₂. *Geochim. Cosmochim. Acta* 65, 695–704.
- Parker, S.R., Gammons, C.H., 2004. Diel concentration cycles of major and trace elements in the Rio Agrio, Argentina. [abstract] Proceedings of the Field Workshop of the 2004 IAVCEI Conference, Caviahue, Argentina, Nov. 20–23, 2004.
- Pedrozo, F., Kelly, L., Diaz, M., Temporetti, P., Baffico, G., Kringel, R., Friese, K., Mages, M., Geller, W., Woelfl, S., 2001. Water chemistry, plankton and trophic status of an Andean acidic lake of volcanic origin in Patagonia. *Hydrobiologia* 452, 129–137.
- Pedrozo, F., Geller, W., Beamud, G., Woelfl, S., Diaz, M., Whitton, B., Wenzel, M.T., Kringel, R., Schimmele, M., Baffico, G., Temporetti, P., Mages, M., 2002. The acidic waters of the crater Copahue-Agrio river-Lake Caviahue system (Patagonia, Argentina). *Verh. Internat. Verein. Limnol.* 28, 112–113.
- Schiff, J., Byrne, R.H., 2004. Determination of SO₄β1 for yttrium and the rare earth elements at $I=0.66$ m and $t=25$ °C—implications for YREE solution speciation in sulfate-rich waters. *Geochim. Cosmochim. Acta* 68, 2825–2837.
- Sholkovitz, E.R., 1995. The aquatic chemistry of rare earth elements in rivers and estuaries. *Aquat. Geochem.* 1, 1–34.
- Takano, B., Suzuki, K., Sugimori, K., Ohba, T., Fazlullin, S.M., Bernard, A., Sumarti, S., Sukhyar, R., Hirabayashi, M., 2004. Bathymetric and geochemical investigation of Kawah Ijen Crater Lake, East Java, Indonesia. *J. Volcanol. Geotherm. Res.* 135, 299–329.
- Varekamp, J.C., 2003. Lake contamination models: evolution towards steady state in stratified lakes. *J. Limnol.* 62 (Suppl. 1), 67–72.
- Varekamp, J.C., Ouimette, A.P., Herman, S.W., Bermudez, A., Delpino, D., 2001. Hydrothermal element fluxes from Copahue, Argentina: a “beehive” volcano in turmoil. *Geology* 29, 1059–1062.
- Varekamp, J.C., Ouimette, A., Kreulen, R., 2004. The magmato-hydrothermal system of Copahue volcano, Argentina. Proc. 11th Intl Conf. on Water–Rock Interaction, WRI-11, vol. 1. Balkema Publishers, Leiden, pp. 215–218.
- Varekamp, J.C., deMoor, M.J., Merrill, M.D., Colvin, A.S., Goss, A.R., Vroon P.Z., Hilton, D.R., in press. The geochemistry and isotope characteristics of the Caviahue Copahue Volcanic Complex, Province of Neuquen, Argentina. Geological Society of America Special Paper “The Neuquen Basin”, Ed. Kay and Ramos (80 pp., accepted pending revisions).
- Verplanck, P.L., Nordstrom, D.K., Taylor, H.E., Kimball, B.A., 2004. Rare earth element partitioning between hydrous ferric oxides and acid mine water during iron oxidation. *Appl. Geochem.* 19, 1339–1354.
- Wendt-Potthoff, K., Koschorreck, M., 2002. Functional groups and activities of bacteria in a highly acidic volcanic mountain stream and lake in Patagonia, Argentina. *Microb. Ecol.* 43, 92–106.
- Wood, S.A., 2003. The geochemistry of rare earth elements and yttrium in geothermal waters. In: Simmons, S.F., Graham, I. (Eds.), *Volcanic, Geothermal, and Ore-Forming Fluids: Rulers and Witnesses of Processes within the Earth*, Soc. Econ. Geol. Spec. Publ., vol. 10, pp. 133–158.
- Wood, S.A., Shannon, W.M., Baker, L., 2005. The aqueous geochemistry of the rare earth elements and yttrium. Part 13. REE geochemistry of mine drainage from the Pine Creek area, Coeur d’Alene River Valley, Idaho, USA. In: Johannesson, K.H. (Ed.), *Rare Earth Elements in Groundwater Flow Systems*, Water Sci. Technol. Libr., vol. 51. Springer, Dordrecht, The Netherlands, pp. 89–110.
- Wood, S.A., Gammons, C.H., Parker, S.R., in press. The behavior of REE in naturally and anthropogenically acidified waters. *J. Alloys Compd.*
- Worrall, F., Pearson, D.G., 2001a. The development of acidic groundwater in coal-bearing strata: Part 1. Rare earth element fingerprinting. *Appl. Geochem.* 16, 1465–1480.
- Worrall, F., Pearson, D.G., 2001b. Water–rock interaction in an acidic mine discharge as indicated by rare earth element patterns. *Geochim. Cosmochim. Acta* 65, 3027–3040.